Methods for CCD Camera Characterization

J.C. Mullikin[1,2], L.J. van Vliet[1], H. Netten[1], F.R. Boddeke[1], G. van der Feltz[1] and I.T. Young[1]

1) Pattern Recognition Group, Faculty of Applied Physics, Delft University of Technology, Lorentzweg 1, 2628 CJ Delft, The Netherlands, *e-mail:* lucas@ph.tn.tudelft.nl
2) Lawrence Berkeley Laboratory, MS: 62-203, One Cyclotron Rd., Berkeley, CA 94720, USA
e-mail: JCMullikin@lbl.gov

ABSTRACT

In this paper we present methods for characterizing CCD cameras. Interesting properties are linearity of photometric response, signal-to-noise ratio (SNR), sensitivity, dark current and spatial frequency response (SFR). The techniques to characterize CCD cameras are carefully designed to assist one in selecting a camera to solve a certain problem. The methods described were applied to a variety of cameras: an Astromed TE3/A with P86000 chip, a Photometrics CC200 series with Thompson chip TH7882, a Photometrics CC200 series with Kodak chip KAF1400, a Xillix' Micro Imager 1400 with Kodak chip KAF1400, an HCS MXR CCD with a Philips chip and a Sony XC-77RRCE.

1. INTRODUCTION

In many biomedical applications there is a need for cameras that satisfy certain specifications. An example is the imaging of small cosmid probes attached to its target using fluorescence in-situ hybridization. The development of direct labeling of fluorescence molecules to the DNA probe greatly reduces the light intensity and requires a camera with a higher sensitivity or a camera that facilitates field integration. It is the scope of this paper to provide the reader with a recipe for testing his or her own camera. Wherever possible we have tried to use simple components available in every microscope laboratory. To illustrate the behavior of some properties, the methods were applied to a few camera systems.

The methods given in this paper describe how to accurately measure the following properties: linearity of photometric response, signal-to-noise ratio (SNR), sensitivity, dark current and spatial frequency response. Linearity of photometric response, which comes with the use of semiconductor sensors, is in some cameras mapped to a nonlinear scale in order to 'gamma-correct' the video signal to produce a linear response on a video display device. This 'gamma-correction' feature needs to be switched off if one requires a linear response. Dark current is defined as the production of electrons per pixel from thermal energy. The SNR per pixel (SNR = 20 log(a/s), with 'a' the signal's amplitude and 's' the standard deviation of the noise) is limited by several noise sources, such as, photon shot noise, readout noise, dark current noise and quantization noise. Spatial frequency response quantifies the sensitivity of the camera to a spectrum of spatial frequencies. Sensitivity relates a camera system's ADC unit to the number incident photons per pixel.

2. METHODS

For all experiments an inverted microscope (Nikon Diaphot TMD) provided the platform from which measurements were made. This microscope was fitted with a 100W halogen lamp (Nikon lamp housing HMX) for epi-illumination (Nikon TMD–EF) and a 50W halogen lamp (Nikon) for bright-field illumination. Both lamps were powered with a stabilized DC power source (Delta Elektronika, Zierikzee, The Netherlands). A shutter (Uniblitz 225L / SD–8800, Vincent Associates, NY) is attached to the microscope just before the epi-illumination lamp mounting bracket. For epi-illumination, a filter block (Nikon DM 510) was used with a green interference filter (Nikon BA 520–560) and an infra-red filter (Nikon) in the emission path. This filter block remained in place for all experiments, including the experiments using bright-field illumination. A c-mount camera adapter mounted to a zoom projection lens (Nikon 0.9–2.25) was placed in the side port of the microscope. Most cameras in this study could be attached to the c-mount. Appendix B lists the cameras used in this study along with manufacturer provided specifications.

0-8194-1468-9/94/$6.00

2.1. Signal-to-noise ratio, Sensitivity and Linearity

The first experiment was designed to measure signal-to-noise ratio, sensitivity and linearity of photometric response of the cameras. The test object in this experiment was a blank slide. A cover slip (RM No.1) was placed on a cleaned slide (Knittel Gläser 76x26 mm) with a drop of immersion oil (Nikon type DF, n_D=1.5150) in between. The oil was allowed to wick-out before placing the slide cover-slip-down in the inverted microscope. A region of the slide with an air bubble trapped under the cover slip was used for focusing with the 20x objective (Nikon PlanApo 20/0.75NA, 160/0.17). The camera zoom port was adjusted for maximum zoom, a reading of 2.25x. A piece of uranyl glass, dimensions 7.5 x 2.5 x 0.3 cm^3, was placed on top of the slide and a black-plastic light shield spanned the slide and uranyl glass. Using epi-illumination the focus on the air bubble was checked and adjusted visually and then with the camera. The air bubble was moved out of the way so that a clear portion of the slide was viewed by the entire region of the camera's detector. One camera owned by our group, listed as Photometrics TH7882 in Appendix B, was used to set the illumination level of the 100W lamp. The level was adjusted such that the mean intensity level of the camera registered slightly less than one-half its maximum value with an exposure time of 1.6 seconds.

With the microscope set up, each camera capable of image integration was mounted on the microscope and a series of images were digitized. For most cameras the integration time was set to 5 seconds and the illumination time was adjusted using the epi-illumination shutter. Shutter times were 0.0, 0.2, 0.4, 0.8, 1.6 and 3.2 seconds, however if the full dynamic range of the camera was not reached in 3.2 seconds of exposure, a longer shutter time was added to the sequence. For all cameras the epi-illumination level was not adjusted[1]. Two images, I_1 and I_2, were acquired at each shutter time indicated, except for the 0.0 s dark level image of which only one image was acquired.

2.1.1. Signal-to-noise ratio:

To calculate signal-to-noise ratio the following equations are used:

$$SNR = 10\log\left(\bar{I}^2 / \mathrm{var}(I)\right) \tag{1a}$$

$$\mathrm{var}(I) = \tfrac{1}{2}\,\mathrm{var}(I_1 - I_2) = \tfrac{1}{2}\left(\tfrac{1}{N-1}\Sigma\left(I_d - \bar{I}_d\right)^2\right) \tag{1b}$$

Where the difference between two images with the same exposure time is $I_d = I_1 - I_2$. The mean of the difference image, $\bar{I}_d$, and its variance, var(I_d), are calculated over a sub-set of all pixels in the image, and normalized by the number of pixels in the sub-image, N.

2.1.2. Sensitivity:

This measure relates a camera system's A/D converter units (ADU) to the number of incident photons captured per pixel†. The number of incident photons is photon flux per pixel times the exposure time. The photon flux at the focal plane of the camera port, Φ_f, was estimated with a Photometrics camera, see Appendix A. Sensitivity is calculated with the following equation:

$$S = \frac{\bar{I} - \bar{I}_{dark}}{\Phi_f A_i t_e} \qquad \text{with} \qquad A_i = \Delta_{x,i}\,\Delta_{y,i} \tag{2}$$

In the numerator of eq. 2, the average pixel value of a dark image is subtracted from the average pixel value of an image acquired with exposure time t_e. The denominator of eq. 2 yields the number of photons that fall in a pixel of area A_i over a time period of t_e. The area of a pixel, A_i, is computed from the sample spacing along the horizontal and vertical axis in the image plane, $\Delta_{x,i}$ and $\Delta_{y,i}$ respectively. The subscript i denotes the image plane. More

---

[1] As an indication of illumination stability, the difference of the intensity level, measured with the Photometrics-1 camera, from the beginning of this experiment to the intensity level after all cameras were tested, was not greater than 1.0%.

† A pixel is not necessarily one CCD well. For most scanned CCD cameras a single "pixel" is one CCD well or some number of binned wells. "Well binning" is where the charge of many wells can be combined before A/D conversion. For video rate CCD cameras a pixel's width along the horizontal scan is related to the sampling rate of the video digitizer board; a higher digitization rate yields a narrower pixel. In the vertical direction a pixel's height is related to, or equal to, the distance between the CCD rows.

commonly, sample spacing is determined in the object plane, however, since the photon flux is measured in the image plane, the plane at which the CCD array is placed, the pixel dimensions must be measured there.

2.1.3. Linearity of photometric response:

Linearity is indicated by the coefficient of regression, R^2, calculated from integration time versus the mean ADU value. These values are taken directly from mean values computed for SNR determination. Below saturation, CCD's are typically photometrically linear, resulting in $R^2 > 0.999$ for a large enough dynamic range.

2.2. Spatial frequency response

This measure shows a camera's spatial frequency response (SFR) to a step-edge object in the focal plane of the microscope. A specially made slide was fabricated at DIMES[2] [DIMES report] for making this type of measurement [Boddeke, Netten et. al]. The slide fabrication steps were as follows: A 100 Å thick layer of chromium was deposited on a slide, then coated with photo-resist and exposed with a pattern which included bars of various widths. The exposure was done using a scanned electron beam. The resist was developed and the exposed chromium layer was etched away completely. Once the resist was removed a cover slip was placed over the chromium layer with a drop of immersion oil in between. A bar pattern with a period of 12.8 μm, a 6.4 μm wide chromium strip blocking all light followed by a 6.4 μm wide blank strip and repeated over a 1x1 mm area, was selected for this experiment.

Since there was a range of $\Delta_{x,i}$ and $\Delta_{y,i}$ sample spacings for the cameras used, an appropriate range of objective and zoom magnification was required to keep the object-plane sample spacing consistent. The smallest $\Delta_{x,i}$ and $\Delta_{y,i}$ camera, cameras using the Kodak (KAF 1400) chip have CCD well dimensions of 6.8 x 6.8 μm, required the lowest overall magnification. The largest $\Delta_{x,i}$ and $\Delta_{y,i}$ camera, the Thompson (TH 7882 CDA) chip with 23 x 23 μm, required the largest overall magnification. Since the sample spacing in the object plane is proportional to $\Delta_{x,i}$ and $\Delta_{y,i}$ and inversely proportional to the overall magnification of the system, one can deduce that the range of magnification must be ~3.4 (23/6.8) fold. This was beyond the range of the zoom lens and therefore required the use of two objectives, a 100x (Nikon Fluor 100/1.3 with a measured NA of 1.21) and a 60x (Nikon PlanApo 60/1.4). The maximum sample spacing in the object plane, $\Delta_{x,o}$ and $\Delta_{y,o}$, should satisfy the Nyquist criterion for the objective used. The maximum spatial frequency passed by an objective with incoherent light is twice the NA divided by the wavelength of the light. Therefore the maximum sample spacing along the x or y-axes should be the wavelength divided by four times the NA:

$$\Delta_{x,o} = \Delta_{y,o} < \lambda/4\,\mathrm{NA} \tag{3}$$

This gives a maximum sample spacing of ~0.096 μm given the wavelength is 0.54 μm and an NA of 1.4 and ~0.111 μm for an NA of 1.21. It was necessary to sample very near the maximum sample spacing since the desired measure was the spatial frequency response of the camera. A camera's spatial frequency response can only be judged over the region which information exists. If the step edge were too finely sampled, then the limiting factor of the system would be the spatial frequency cut-off of the objective. If the system does not sample finely enough then aliasing would occur, corrupting the data. For each camera the zoom and the objective were chosen to give a sample spacing near 0.1μm. The true sample spacing was later measured from the image of the bar pattern.

The slide was placed in the Nikon microscope with one of the two objectives coupled to the slide with immersion oil. On the other side of the slide the condenser (Nikon Achromat/Aplanat Condenser NA 0.1 to 1.35) was also coupled with immersion oil. Filters placed after the halogen lamp and before the condenser included a GIF (Nikon 40 mm Green Interference Filter) and a neutral density filter. The intensity of the lamp was adjusted to a mid-range level (an absolute intensity level was not crucial for this experiment). The microscope was adjusted for Köhler illumination and the zoom was adjusted to reach the required sample spacing. For each camera, images were acquired of a portion without bars (a clear portion of the slide), another with the shutter closed (a dark image), and two more with the bars aligned parallel to the rows and parallel to the columns of the CCD.

Each bar image, I_h and I_v, was corrected for systematic shading — variations in image intensity due to nonuniform illumination, sensitivity and dark current. This is accomplished with the following equation:

---

[2]DIMES (Delft Institute for Microelectronics and Sub-Micron Technology, Delft, The Netherlands) is a government funded research institute at the Delft University of Technology. It is specialized in design and fabrication techniques for submicron technology.

$$I_{corrected} = \frac{I - I_{dark}}{I_{blank} - I_{dark}} \quad (4)$$

where I_{blank} is the image from the blank portion and I_{dark} is the dark image[3]. The corrected image, $I_{corrected}$, could be rescaled, however absolute intensity measurements are not needed in the following measurements and since the result is stored in single precision floating point variables, rescaling would not affect the results. A bar-edge located nearest the center of the camera's detector was selected for measuring the modulation transfer function (MTF). A 32 pixel wide region centered over this edge (~1.6μm to either side of the edge) was selected for further processing, see figure 1a. This region was rotated some multiple of 90° into a new image such that the edge transition was from dark to bright along a horizontal line. This image was interpolated to a sample spacing 8 times finer than the original in the horizontal direction, see figure 1b, using a spline interpolation routine [Press]. A 1-D derivative-of-Gaussian kernel with coefficients (σ=1.5) was convolved with the interpolated image along each horizontal line.

The result is a nearly perfect impulse response of the camera perpendicular to the direction of the bars [Young], which unfortunately includes noise, see figure 1c. If the edge were perfectly aligned and free of defects, an ensemble average in the vertical direction would improve the signal-to-noise ratio by the square root of the number of lines averaged. However, since the edge does not satisfy either of the given prerequisites the derivative image must be corrected. This correction involves shifting each line so that the edge is aligned with the central pixel. Once again, noise produces uncertainty in the location of the edge. By applying a smoothing filter to the line and detecting the maximum value position the uncertainty of the edge position is reduced [Canny]. Our method used a Gaussian shaped smoothing kernel with coefficients (σ=7.9).

Once the lines are shifted, see figure 1d, an ensemble average of all lines produce a 1-D impulse response, see figure 1e. The Fourier transform of the impulse response gives the system's overall MTF_S in figure 1f. By comparing the MTF_S with the MTF of an ideal optical system [Born, Williams], i.e. the MTF of a perfectly focussed diffraction limited optical system using incoherent light, one can deduce the camera's spatial frequency response. All CCD cameras exhibit a fundamental sinc-shaped degradation in spatial frequency response since each CCD well collects photons uniformly over its surface (spatial integration).

Other methods for characterizing the SFR of CCD cameras include a holographic method [Marchywka] and a microscope based method using fluorescent microspheres [Hazra]. The holographic method requires a laser-based testing apparatus. The advantage of this system is that it can test the SFR to beyond the Nyquist rate limitation imposed by the CCD array. Likewise, Hazra et al. achieve extended spatial frequency information by acquiring multiple, sample-shifted target images. These multiple images are recombined into one sub-sampled image, which allows system characterization beyond the Nyquist rate. The step edge method described in this paper characterizes the system up to the Nyquist limit.

2.3. Dark Current

Electrons are not only produced by photons, but also by thermal energy. Dark current is defined as the rate of induced electrons per pixel from all sources other than photons. Since thermally induced photons are the main contributor to dark current, cooling the camera reduces this unwanted electron source. Measuring dark current is relatively simple and does not require an optical setup.

We performed dark current measurements after the cameras were on for more than an hour. Photons were kept from reaching a camera's CCD sensor by capping its lens port with a black mask. Planned integration times were 1, 10 and 100 seconds, however HCS and Xillix had maximum integration times of 50 and 20 seconds respectively.

Figure 1 (next page): a) Image of the bar pattern with a 12.8μm period cycle. A 32 pixel wide segment is selected from the middle of the image. **b)** The image region selected from figure 1a is interpolated by a factor of 8 in the x-direction using splines to produce this image. The scale in this figure is not equal along the x and y-axes (see scale bars). The roughness of the edge is clearly visible. **c)** One X trace through the differentiated image. **d)** The edge roughness is removed by shifting the lines. The result is shown here. **e)** The result of averaging all X traces of figure 1d together. **f)** The Fourier transform of the result shown in figure 1e.

[3]This expression and all calculations hereafter are in single precision floating point including the real and imaginary parts of complex numbers. Fourier transforms are calculated internally with double precision numbers, however the input and output are single precision floating point numbers.

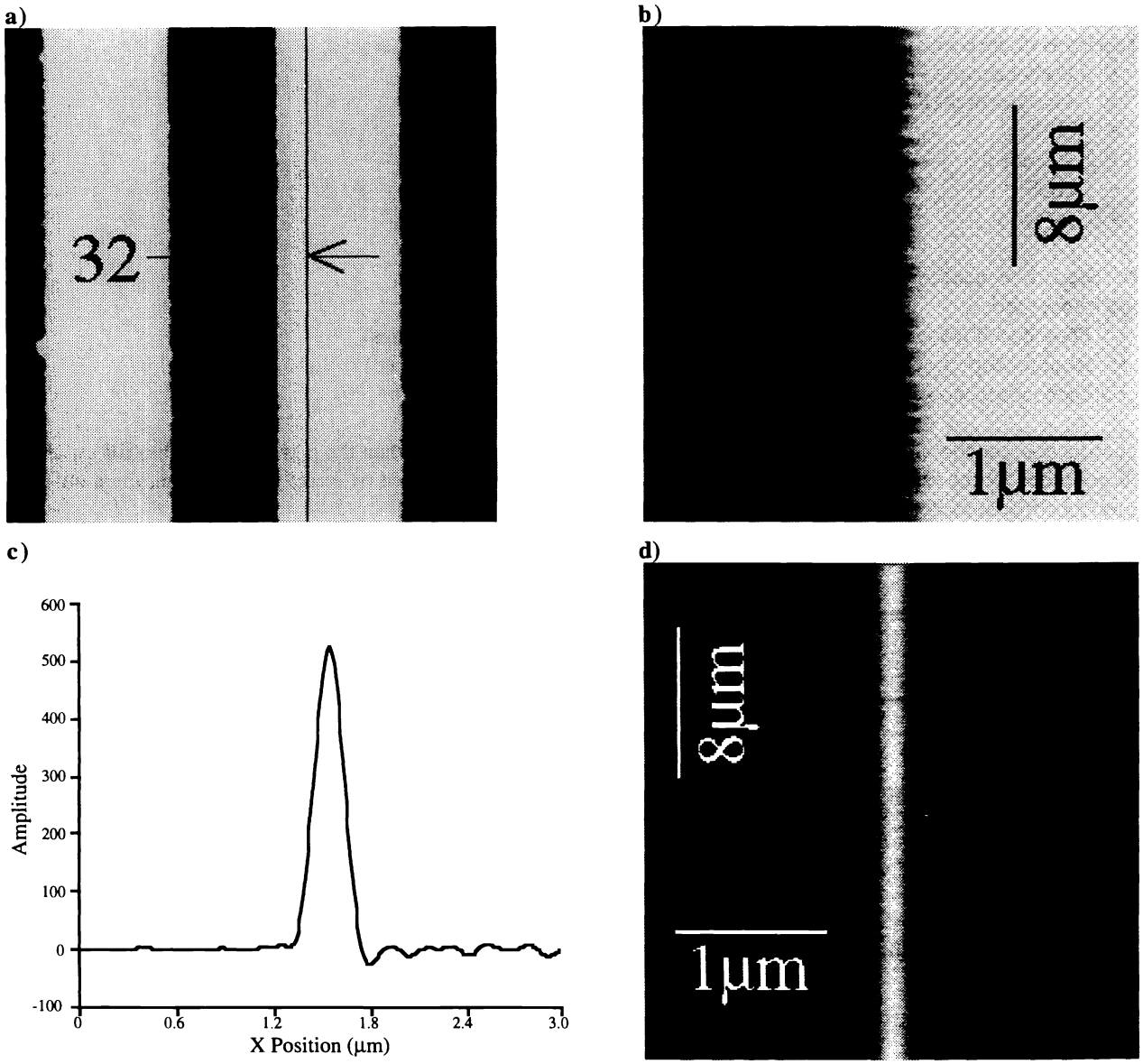

3. RESULTS

All methods of the previous section were used to characterize the following cameras:

- Photometrics (TH7882) Thompson chip TH 7882
- Photometrics (KAF1400) Kodak chip KAF1400
- Xillix Kodak chip KAF1400
- Astromed P86000 chip
- HCS Philips chip
- Sony Sony XC-77RRCE

3.1. Signal-to-noise ratio

Noise sources are:

- Photon shot noise (quantum nature of light which obeys Poisson statistics)
- Readout noise (preamplifier noise which increases rapidly with readout rate)
- Dark current noise (dark current that has a quantum nature as well)

Assuming that the photon shot noise dominates over the other noise sources when the photo sites (wells) fill up, the SNR is limited by the capacity of the well, N_c. Because all electrons are created by exactly one photon, the number of electrons N_e obeys Poisson statistics as well.
For each signal level (N_e) the SNR per single pixel is limited by:

$$SNR = 20\log\left(N_e/\sqrt{N_e}\right) = 10\log\left(N_e\right) \tag{5}$$

Using the relation:

$$\#\text{ADU} = N_e\, G \tag{6}$$

with G the electronic gain we get for the maximum SNR the following expression

$$SNR_{\max} = 10\log\left(\left(2^{\#bits}-1\right)/G\right) = 10\log\left(2^{\#bits}-1\right) - 10\log(G) \tag{7}$$

We notice that the maximum SNR can be increased by using an AD converter with more quantization levels or by reducing the electronic gain G. Reduction of the electronic gain does not help below a certain level where the number of electrons needed to produce a full output in ADU's is larger than the well capacity for electrons, $(2^{\#bits}-1)G^{-1} \geq N_c$.
Knowing this, we have to realize that a measure of SNR for a particular camera only makes sense if the value is related to the maximum SNR for the number of electrons per well (cf. table 1).

Table 1: SNR's for various intensity levels (t_e). For each exposure time we list the measured SNR and the ideal SNR. The maximum SNR, SNR_{max}, is limited by the Poisson distribution of the electrons producing a maximum output signal, N_c.

exposure time (s)	0.2	0.4	0.8	1.6	3.2	SNR_{max}
Photometrics (Th 78882)	41/43	44/46	49/49	52/52		56
Xillix	22/32	28/35	34/38	39/41	43/44	47
Astromed	42/42	46/45	49/48	52/52	55/55	58
HCS	17/38	23/40	29/43	38/46	40/50	51
Sony	30/35	35/37	39/40	43/43	39/47	49

State-of-the-art cameras such as a Photometrics camera based on the KAF 1400 CCD produce a SNR that is photon limited (equal to the ideal SNR) over the entire dynamic range of the output signal in ADUs (cf. Figure 2).

3.2. Sensitivity

Sensitivity S can also be written as

$$S = QE\ G\ F\ \tau_w \tag{8}$$

with QE, the quantum efficiency, G, the number ADU's per electron (electronic gain), F the fraction of the pixel that is photo sensitive (filling factor), and τ_w, transmission coefficient of the camera window

Sensitivity can be increased by increasing the electronic gain of the camera. CCD's have a higher quantum efficiency for red light than for blue light. In the infra red (IR) region of the spectrum the quantum efficiency approaches 100% whereas in the ultra violet (UV) the quantum efficiency is virtually zero. This has important consequences for the sensitivity.

For the Photometrics KAF 1400 camera we estimated the variance in the image I from a difference image. A photon limited camera system has a linear relation between the measured variance and the average image intensity (cf. fig.3).

$$\mathrm{var}(I) = G\left(\bar{I} - \bar{I}_{dark}\right) + \mathrm{var}\left(I_{dark}\right) \tag{9}$$

with $I = s\ (t_{exposure}\ A_i\ \Phi)$.

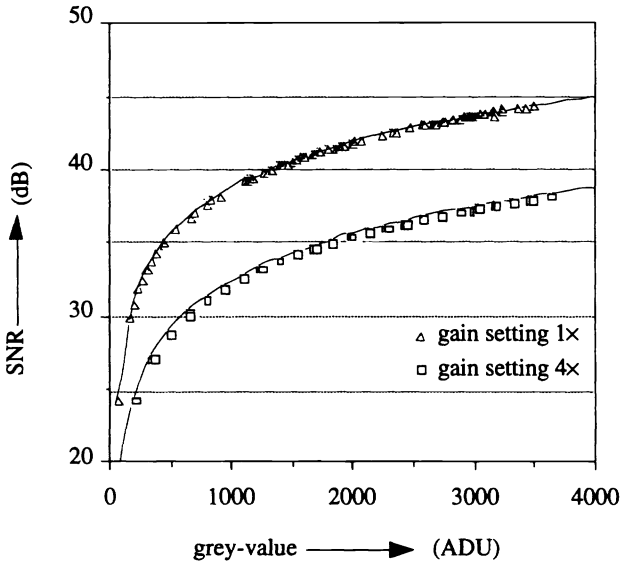

Figure 2: The SNR of an empty (blank) image for two gain settings as a function of the corrected (for dark current and bias) average pixel value for the Photometrics KAF1400 camera. The solid lines show the predicted SNR in case of photon shot noise only (12 bit ADC and electronic gain $g_{1\times}$=0.126 and $g_{4\times}$=0.539).

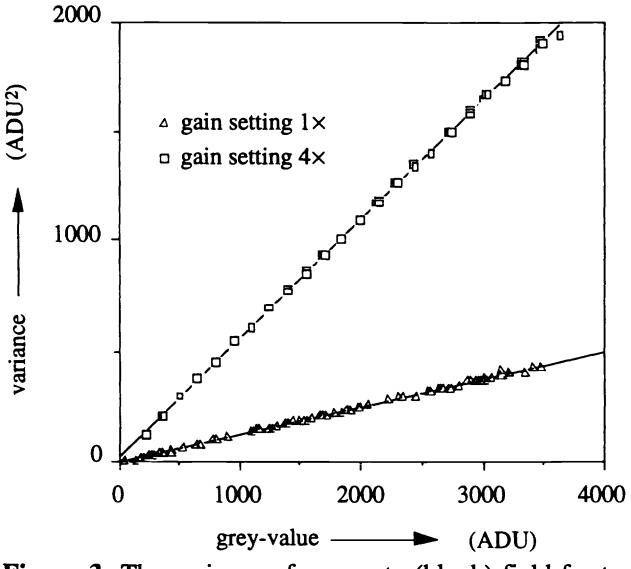

Figure 3: The variance of an empty (blank) field for two gain settings as a function of the corrected (for dark current and bias) average grey-value. Fitting a straight line to both the data sets (R^2=1.000) yields an electronic gain of $g_{1\times}$=0.126 e^{-1} ADU and $g_{4\times}$=0.539 e^{-1} ADU respectively.

Table 2: Electronic gain (ADU response per electron) measured with an constant photon flux that corresponds to an equivalent "electron flux" of 186 e s^{-1} μm^{-2} on the Photometrics TH7882 camera and an exposure time of 1.6 s. For the Xillix camera the upper eight out of ten bits are considered. This action reduced the sensitivity by a factor of four. Both Photometrics cameras and the Astromed support other system gains (four times higher for the Photometrics and eight times higher for the Astromed).

	G (ADU $(e^-)^{-1}$)	I / I_{max}
Photometrics (TH 7882) 1x gain	0.011	1742 / 4095
Photometrics (KAF 1400) 1x gain	0.126	n.a.
Photometrics (KAF 1400) 4x gain	0.539	n.a.
Xillix	0.0052	72 / 256
Astromed	0.103	14859 / 65535
HCS	0.0021	93 / 256
Sony	0.0039	n.a.

I_{dark} is called a dark image. The only difference between a dark image and a normal exposure is that for a dark image the camera shutter stays closed. Var(I_{dark}) or dark noise contains contributions of readout noise and dark current noise. The slope of the function equals the electronic gain of the camera. The Photometrics KAF 1400 in standard operation mode yields an electronic gain of $g_{1\times}$=0.126 e^{-1}ADU (in the 4× gain mode the electronic gain becomes $g_{4\times}$=0.539 e^{-1}ADU). The electronic gain for other cameras is given in table 2. The photon flux Φ_f was kept constant during these experiments. The photon flux can be calculated using the method of Appendix A. The images acquired with an exposure time of 1.6 seconds are used to calculate the sensitivity.

To estimate the sensitivity we need knowledge about the transmission coefficient of the camera window ($\tau_w \approx 1$), the fill factor (KAF1400 $f \approx 1$) and the quantum efficiency for the wavelength being used (CCD specifications).

3.3. Linearity

CCD cameras exhibit linear photometric response for almost their entire dynamic range. This is measured by fitting a linear regression line to the intensity data for various exposure times and recording coefficient of regression (R^2). The coefficient of regression (R^2) results are shown in table 3. (Note: intensity results for the Photometrics 3.2 second exposures are excluded. Including these results gives R^2 = 0.995767)

Table 3: Coefficient of regression as indicator of linearity.

	Coefficient of regression R^2
Photometrics (TH 7882)	0.999899
Photometrics (KAF1400)	1.00000
Xillix	0.999984
Astromed	0.999800
HCS	0.999937
Sony	0.999612

3.4. Spatial frequency response

Depicted in figure 4 are the cameras' overall impulse response, or likewise spatial frequency response (SFR), across CCD rows and columns. Also depicted is the theoretical MTF of the objective. All responses are normalized such that the DC value is unity. Below is a table which lists the objective, zoom setting and measured sampling spacing.

Table 4: Microscope configuration and measured sample spacings for each camera.

	Objective	Zoom	Row Spacing (μm)	Column Spacing (μm)
Photometrics TH7882	100	2.25	0.1057	0.1062
Xillix	60	1.15	0.0989	0.0986
Astromed	100	2.25	0.1073	0.1072
HCS	60	1.32	0.1979	0.1142

3.5. Dark Current

Dark current reduces the dynamic range of a camera because precious well space is occupied by non–specific electrons. Since thermally induced electrons are the main contributor to dark current, cooling the camera reduces this unwanted electron source. Some two-phase CCD chips such as the KAF 1400 support a special integration mode called multi phase pinning (MPP). Operation in MPP mode reduces the dark current up to two orders of magnitude at the expense of a lower well capacity. A cooled KAF 1400 in MPP mode (Photometrics KAF 1400 at –37°C) produces a dark current of 0.002 ADU s^{-1} $pixel^{-1}$ (0.0003 e s^{-1} μm^{-1}). Without cooling, but using a special accumulation mode, another chip of the same type (Xillix's Micro Imager 1400, Vancouver BC, Canada) produces a dark current of 0.12 ADU s^{-1} $pixel^{-1}$ (0.49 e s^{-1} μm^{-1}). The dark current measurements for the various cameras are listed in table 5.

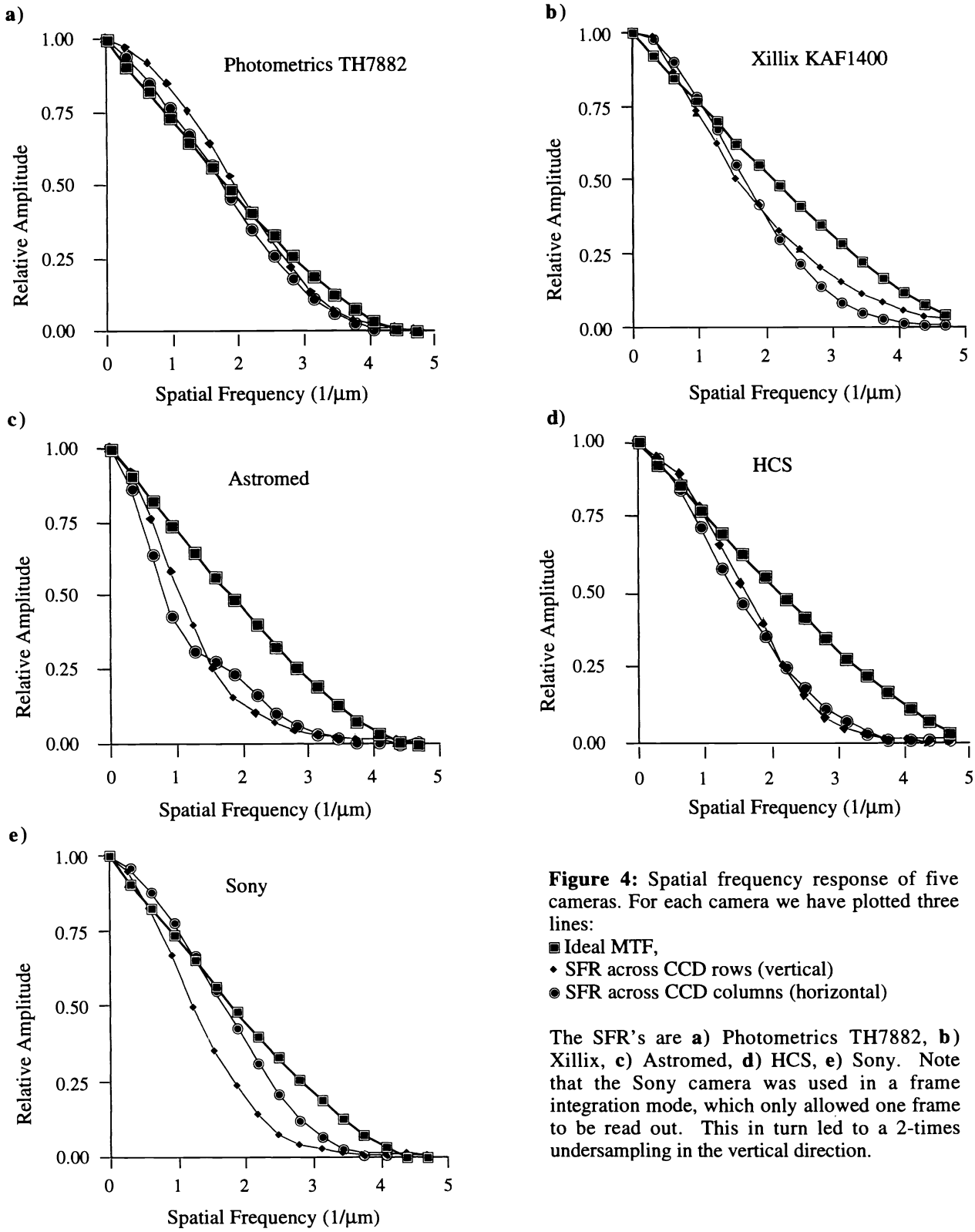

Figure 4: Spatial frequency response of five cameras. For each camera we have plotted three lines:
- ■ Ideal MTF,
- ◆ SFR across CCD rows (vertical)
- ◉ SFR across CCD columns (horizontal)

The SFR's are **a)** Photometrics TH7882, **b)** Xillix, **c)** Astromed, **d)** HCS, **e)** Sony. Note that the Sony camera was used in a frame integration mode, which only allowed one frame to be read out. This in turn led to a 2-times undersampling in the vertical direction.

Table 5: Dark current in ADU s^{-1} $pixel^{-1}$. From the dark current, electronic gain and pixel size we calculate the "dark electron flux" Φ_{dark}.

	dark current (ADU s^{-1} $pixel^{-1}$)	exposure time (s)	equivalence Φ_{dark} (e s^{-1} μm^{-2})	temperature °C
Photometrics (TH 7882)	420 10^{-3}	100	72 10^{-3}	–34.8
Photometrics (KAF 1400)	1.9 10^{-3}	1000	0.33 10^{-3}	–42
Sony (w/ dark suppression)	43 10^{-3}	40	46 10^{-3}	20
Astromed	5.6	100	0.11	–46
Xillix	0.12	20	0.49	20
HCS	2.8	50	8.9	20

4. DISCUSSION

As expected, all CCD cameras tested exhibit a linear photometric response.

The slow-scan CCD cameras (Photometrics and Astromed) have a SNR that is photon limited over the entire range over operation. Xillix' (8MHz. readout) SNR becomes photon limited for signals larger than 50% of its dynamic range. For both video cameras the readout noise dominates. The maximum signal-to-noise ratio depends on the well capacity of an individual pixel. The well capacity is proportional to the pixel size. The SNR can be increased by on-chip binning. There exists a trade-off between SNR and spatial resolution (pixel size).

The sensitivity is dominated by the electronic gain. Sensitivity can be increased by increasing the gain in exchange for a lower dynamic range, or by selecting an A/D converter with more bits. On-chip binning does not change the sensitivity.

Dark current of cooled cameras allows long integration times. The Sony camera subtracts the average dark current. However, after several seconds of integration time, the image shows hot-spots due to impurities and irregularities of the Silicon.

The spatial frequency response (SFR) of the Astromed is severely degraded by the vibrations of the fan mounted on the camera head (this is solved in later versions of this system). The Sony – an interline transfer CCD – shows a clear discrepancy between the SFR across the rows and the columns of the CCD. The SFR's across rows and columns of the HCS camera are almost the same. This indicates that its shape is independent of the video related electronics.

We believe it is to early to draw definitive conclusions from the results presented in this report. Looking at the results one should be aware of the fact that several cameras have programmable options that have not been (or could not be used) used to there full extent. Especially the cameras with variable gain (sensitivity) settings deserve more attention.

LITERATURE

[Boddeke] F.R. Boddeke, Autofocusing in microscopy, Mater's thesis, Delft University of Technology, 1992.

[Born] M. Born and E. Wolf, Principles of optics, sixth edition, Pergamon Press, 1959.

[Canny] J. Canny, A computational approach to edge detection, IEEE PAMI–8(6), pp. 679–698, 1986.

[DIMES] DIMES annual report 1991.

[Hazra] R. Hazra, C.L. Viles, S.K. Park, S.E. Reichenbach and M.E. Sieracki, Model-based frequency response characterization of a digital-image analysis system for epifluorescence microscopy, Applied Optics, Vol. 31, No. 8, pp. 1083-1092, 1992.

[Marchywka] M. Marchywka and D.G. Socker, Modulation Transfer function measurement technique for small-pixel detectors, Applied Optics, Vol. 31, No.34, pp. 7198-7213, 1992.

[Netten] H. Netten, L.J. van Vliet, P. de Jong, F.R. Boddeke, and I.T. Young, ICAS: Scanner and analyzer for fluorescent microscopy, Cytometry, Supplement 5, pp. 70, 1991.

[Press] W.H. Press, B.P. Flannery, S.A. Teukolsky, and W.T. Vetterling, Numerical recipes in C, Cambridge University Press, 1988.

[Williams] C.S. and O.A. Becklund, Introduction to the optical transfer function, John Wiley, 1989.

[Young] I.T. Young, H. Zagers, L.J. van Vliet, J.C. Mullikin, F.R. Boddeke, H. Netten, Depth-of-Focus in Microscopy, Proceedings of 8SCIA, Tromsø, Norway, pp. 493-498, 1993.

ACKNOWLEDGMENTS

We gratefully acknowledge Peter de Jong for his technical expertise. Hans Vrolijk, Hans Tanke, Nico Verhoeven and Willem Sloos from the Sylvius Laboratory at the University of Leiden for their useful discussions on the subject. And of course this would not have been possible without the generous cooperation of BDS for providing us with the Xillix and HCS cameras. Special thanks to two of their people: Peter den Engelse who was a big help capturing images with the Xillix and HCS cameras and Nellie Schipper who initiated this first camera test. Last but not least we thank Leica b.v. in Rijswijk for providing us with the Astromed system. This work is partially supported by The Netherlands' Project Team for Computer Science Research, SPIN (Project Three-Dimensional Image Analysis), The Netherlands Foundation for Medical Research, NWO–MW grant 900–538–016, and Imagenetics in Naperville Illinois.

APPENDIX A: CONVERSION FROM PHOTONS TO ADC UNITS

A CCD camera integrates photon flux in the image plane during exposure. After digital readout, each pixel contains a value proportional to the number of incident photons on that pixel plus some offset due to bias and dark current. In this appendix we explain how to compute photon flux via statistical methods.

To apply statistical methods for measuring photon flux, noise sources must be identified. Main sources of noise in an image are: photon noise (photons are Poisson distributed), readout noise (mainly produced by the pre–amplifier and dependent on the readout rate), quantization noise of the analog-to-digital converter, and dark current noise. For a slow scanned CCD camera such as the Photometrics (a readout rate of 500 kHz., 12 bit ADC, and cooled to –35 degrees) the photon noise dominates significantly over the other noise sources when the wells on the CCD are sufficiently filled. By measuring the level of photon noise with respect to the mean image intensity we can determine photon flux, and from this a camera's sensitivity can be determined.

The conversion of photons into ADU's obeys eq. A1

$$I = N_e\, G = N_p\, QE\, \tau_w\ F\, G \tag{A1}$$

with N_p the number of photons hitting the surface of one well, N_e the number of free electrons of the same well, QE is the CCD's quantum efficiency for the incident wavelength, τ_w is the transmission coefficient of the camera window, G is the conversion factor from electrons into ADU's and F is the CCD's filling factor (100% for the KAF1400 chip).

Typical values of the QE for front illuminated CCD's are around 50% (higher in the red and lower in the blue). The camera window can be made from quartz and coated to reduce reflections. High quality cameras are being delivered with these special coatings with transmission coefficients near one (no loss).

For a Poisson distributed stochastic signal N_e and its transformed version I (see eq. A1) we can derive the unknown system parameters such as the overall conversion factor from photons to ADU's and the photon flux. Statistical properties of a stochastic signal can be replaced by ensemble averaging when the signal is stationary. For this experiment this translates into a constant photon flux in time and independent of the position. The variance of a single pixel in ADU's cannot be estimated by the variance within one image due pixel variability. This variability can be suppressed by using half the variance of a difference image where the two exposures I_1 and I_2 are two realizations of the same signal. The variance of the difference image is estimated by taking the mean over a uniformly illuminated field.

Using eq.(A1) the pixel's variance in ADU's can be expressed in the pixel's variance in photons

$$\mathrm{var}(I) = G^2\, \mathrm{var}(N_e) \tag{A2}$$

Using a property of Poisson distributed signals we derive the following relationship where the expectation value for a pixel's intensity in ADU's can be estimated by the average over a uniformly illuminated field.

$$\mathrm{var}(N_e) = N_e = \frac{\bar{I}}{G} \tag{A3}$$

From the above two equation we derive the conversion factor G from electrons into ADU's as follows:

$$G = \frac{\mathrm{var}(I)}{\bar{I}} = \frac{\mathrm{var}(I_1 - I_2)}{2\bar{I}} \tag{A4}$$

The overall conversion factor equals the camera's sensitivity.

$$QE\ \tau_w\ G\ F = S \tag{A5}$$

The photon flux Φ_f in the image plane (see eq. 2) is therefore given by

$$\Phi_f = \frac{\bar{I} - \bar{I}_{dark}}{A_i\, t_e} \left(QE\ \tau_w\ F\, G\right)^{-1} \tag{A6}$$

This method does not work for all cameras because noise terms other than photon noise may dominate. However, once the photon flux is determined using a suitable camera, we can achieve our goal of measuring a camera's sensitivity by keeping the photon flux fixed and filling in the blanks of eq.(2).

For two out of the four cameras the photon noise dominates: the Photometrics TH7882 and Astromed cameras. Due to different system settings they have a different overall conversion factor. The photon flux was kept constant for the duration of the measurements.

Table A: Camera's conversion factor (electronic gain) and "electron flux" measured with an exposure time of 1.6 s.

	G	Φ (e s^{-1} μm^{-1})
Photometrics TH7882	0.011	186
Astromed	0.102	189

APPENDIX B: CAMERA SPECIFICATIONS

Manufacturer	Photometrics	Photometrics	Xillix	Astromed	HCS	Sony
type / model	CC200 Series	CC200 Series	Micro Imager	TE3/A	MXR CCD	XC-77RRCE
serial number			X 0012	1014	5012939109132	
year	1988	1991	1991	1991	1991	1992
CCD type	TH7882 Thompson	KAF 1400 Kodak	KAF 1400 Kodak	P86000	NXA1011 Philips	PA-93
dimensions	384 x 576	1320 x 1035	1320 x 1035	578 x 385	604 x 576	756 x 581
pixel size (μm)	23.0 x 23.0	6.8 x 6.8	6.8 x 6.8	22.0 x 22.0	10.0 x 15.6	11.0 x 11.0
cooling method	Peltier –36.8°C	Peltier –42°C	None	Peltier air -46°C	Peltier air –5°C	None
IR filter	No	No	Yes	No	Yes	Yes
binning	Yes	Yes	Yes	Yes	No	No
color	No	No	No	No	No	No
interface	12 bits	12 bits	10 bits	16 bits	CCIR + TTL	CCIR + TTL
host computers	VME, MacII	VME, MacII	AT bus	IBM-PC	video	video
coating	Yes	Yes	No	Yes	No	No
gamma	No	No	No	Yes	Yes 1/0.45	Yes 1/0.45
auto gain	No/(1x,4x)	No/(1x,4x)	No (electronics)	No / Variable	No / Variable	No / Variable
readout rate	500 kHz	500 kHz	(0.5,1,4,8) MHz	20 kHz	14 MHz	14 MHz